A High Performance and Low Latency Deep Spiking Neural Networks Conversion Framework

Anonymous Author(s)
Affiliation
Address
email

Abstract

Spiking Neural Networks (SNN) are promised to be energy-efficient and achieve Artificial Neural Networks (ANN) comparable performance through conversion processes. However, a converted SNN relies on large timesteps to compensate for conversion errors, which as a result compromises its efficiency in practice. In this paper, we propose a novel framework to convert an ANN to its SNN counterpart losslessly with minimal timesteps. By studying the errors introduced by the whole conversion process, an overlooked inference error is reveald besides the coding error occured during converting. Inspired by the quantization aware traning, a QReLU activation is introduced during training to eliminate the coding error theoretically. Furthermore, a buffered non-leaky-integrate-and-fire neuron that utilizes the same basic operations as in conventional neurons is designed to reduce the inference error. Experiments on classification and detection tasks show that our proposed method attains ANNs level performance using only 16 timesteps. To the best of our knowledge, it is the first time converted SNNs with low latency demonstrate their capability to achieve high performance on nontrivial vision tasks. Source code will be released later.

1 Introduction

Recently, Spiking Neural Networks (SNN) have attracted a great deal of researchers' attention due to their essential advantages, such as spatio-temporal information processing capability and energy-efficient with low power consumption. Unlike conventional Artificial Neural Networks (ANN) communicating with every neuron between layers during every inference step, SNN only passes sparse events when particular neurons are fired. This compute-on-demand property of SNN is very friendly to low-power hardware, and suitable for neuromorphic platforms, such as event-based camera [11] and brain-inspired chips [32]. Such dedicated bionic systems can significantly reduce memory usage and energy consumption, which is very appealing to a wide range of applications like autonomous mobile robots.

Despite the promising characteristics, it is still a challenging problem to train high-performance deep SNNs for practical tasks. Directly applying the backpropagation approach is infeasible because of the non-differentiable nature of the spike activity. Taking advantage of the ANN's success, conversion methods have been proven to be a very promising direction in achieving high performance SNN. Cao et al. [4] first convert ANNs to SNNs by demonstrating the relationship between spiking neuron and ReLU function for rate-based methods. Diehl et al. [9] propose a weight normalization approach to mapping weights from ANN to SNN. Later, Rueckauer et al. [39] give a theoretical analysis on ANN-SNN conversion. A reset-by-subtraction IF neuron is proposed to better handle the accuracy degradation during the conversion. They also propose the weight normalization algorithm that uses percentile function instead of max value to achieve better performance. Kim et al. [23] propose a channel-wise normalization to further reduce the performance gap between ANNs and SNNs .

Submitted to 36th Conference on Neural Information Processing Systems (NeurIPS 2022). Do not distribute.

Although great progress has been made, those converted SNNs suffer from *accuracy-latency trade-off* [9, 31]. As a result, the converted SNNs need longer time to achieve comparable precision with their counterpart ANN during inference and compromises the efficiency in practice. To deal with this problem, hybrid methods [37, 36] are proposed to further finetune a converted SNN with approximated gradients to decrease the inference time. On the other hand, for the theoretical training gaps between ANNs and SNNs, Ding et al. [10] propose Rate Norm to better choose the scale factor and introduce extra loss to decrease the latency. Deng and Gu [8] utilize training samples to transfers the weights to the target SNN by combining threshold balance and soft-reset mechanisms. However, these works only focus on reducing the errors introduced by mapping feature values to spike trains.

With an in-depth analysis of the entire coversion process, we recognize two types of conversion errors, namely coding error and inference error, that degrade the performance of SNN. As other conversion approaches mainly focus on the coding errors, our motivation is to reduce both the coding and inference errors. Inspired by the analysis in Rueckauer et al. [39], we notice that the SNN with step function resembles quantized ANNs. By establishing a strict equivalency between spiking neuron and quantized activation function, the coding error can be eliminated completely under limited timesteps. Further, we observe that the assumption in rate-based conversioin is inconsistent with the actual neuron behavior and the SNN's dynamics during the inference. Most of the previous conversion-related literature overlook this problem, which limits the performance of the algorithms and leads to longer simulation time to achieve comparable results of the original ANN.

In this paper, we propose a novel High Performance Conversion (HPC) method to drastically close the gap between ANNs and SNNs. Specifically, a QReLU activation is proposed to eliminate the coding error. Since QReLU is applied to the ANN training phase, no extra effort is required during the conversion. Besides, a noval buffered non-leaky IF neuron is designed to compensate for the inference error and retain SNN's efficiency during inference. Utilizing a new form of activation function and novel efficient spiking neuron, SNN obtained by our proposed approach achieves high performance and low latency simultaneously. With only 16 timesteps, HPC achieves state-of-the-art performance across classification and detection tasks. Our major contributions are summarized as:

- An overlooked inference error is discovered. The conversion errors including both coding errors and inference errors are theorically analized to clearify the reason of performance degration during conversion.
- A novel high performance conversion method is proposed to deal with the two types of conversion errors. The coding errors are eliminated completely in theory and the inference error problem is relieved to a great extent.
- Comprehensive experiments on different tasks demonstrate the efficacy of the proposed method. To the best of our knowledge, it is the first time converted SNN achieves ANN level performance while maintaining high efficiency and low latency across various tasks.

2 Related Work

Up to now, there exist two main categories of supervised training strategies for SNN: approximated error backpropagation methods, and conversion methods.

Our proposed work is mainly related to ANN-SNN conversion methods with rate-based coding [9, 35, 4, 39]. The goal of conversion approaches is to remain the high performance of ANN in SNN framework. Recently, Xing et al. [44] extend the territory of conversions by adding supports to more structures such as softmax activation and residual block. Instead of using longer timesteps to aproximate ANN accurately, conversion errors are analized and compensated by adjusting the parameters of converted SNN [27]. Rate Norm is proposed [10] to better choose the scale factor. Deng and Gu [8] utilize training samples to transfers the weights to the target SNN by combining threshold balance and soft-reset mechanisms. As a general approach, Kim et al. [23] show that conversion can be applied to detection tasks. However, only coding error are considerd in those work. We notice that the inference error or "unevenness error" is described in the parallel work [3]. However, the "unevenness error" is ignored during the analysis of conversion error in their work.

Other researchers [2, 29, 21] try to approximate the gradient to train the SNN by replacing the threshold function with other functions. A comprehensive summary of surrogated gradient backpropagation methods can be found in [30]. Huh [20] introduce differentiable synapse and neuron models to

SNNs. Since spike trains are normaly sparse, gradients in SNNs are naturelly sparse compared to traditional ANNs. An sparse spiking gradient descent approach is introduced [34] to speed up the backpropgation. To enable very deep spiking neural network, modified residual module with element-wise functions [14] is proposed to mimic directly gradient path of ResNet [17]. Rather than compute the approximated gradient, a neuron with extra inner state is introduced in [42] to estimate the gradient. Different from [42], the buffered neruon proposed in this literature utlizes extra inner state to compensate for inference error. Backpropagation trained SNNs show the potential of achieving ANN level performance. However, extra efforts are required to train the SNN properly, making it hard to train and limit its application on real world tasks.

Recently, combined methods [37, 36] emerges to alleviate the drawbacks that conversion methods require larger timesteps to achieve competative performance. These methods often contain two steps: conversion and fine-tuning. The SNN converted in the first step is served as a weight initialization for a further fine-tuning procedure using backpropagation. With the help of roughly mapped weights, several epochs of fine-tuning yield nearly loss-less performance with fewer timesteps [37]. However, compared to conversion methods, extra efforts are required to fine-tune the SNN. Also, the backpropagation imposes additional limitations to the hybrid approach, which further restrains its application.

3 Methods

In this section, we first analyse the theoretical equivalency and gaps between a target SNN and an original ANN. Then, a quantized activation is proposed to minimize the coding error during the conversion. A buffered non-leaky IF neuron is presented to reduce the inference error. Finally, we integrate the proposed conversion framework to further decrease the difference between SNN and ANN.

3.1 Theoretical Errors and Analysis

Following Rueckauer et al. [39], we here illustrate the equivalency between SNN and ANN and introduce two types of errors when using the conversion methods with rate-based coding. The target SNN shares a similar overall architecture with the original ANN except two significant discrepancies. First, neurons in the SNN communicate with each other by spike trains $S(t)$ where $S(t) \in \{0, 1\}$ for each timestep $t \in \{1, ..., T\}$, while the activation functions in ANN utilize real-value. T is the total timesteps. Second, a non-leaky integrate-and-fire (IF) neuron is used instead of the ReLU activation in conventional ANN. The membrane function of the non-leaky IF neuron j can be described as:

$$V_j(t) = V_j(t-1) + V_{th} \sum_{i \in \mathcal{N}_j} w_{ij}^s S_i(t) - V_{th} S_j(t). \tag{1}$$

where $V_j(t)$ is the membrane potential of the jth neuron and t is the timestep. $\mathcal{N}_j$ is the set of all input neurons in the last layer connecting to jth neuron. w_{ij}^s is the weight and connection strength between the input ith neuron and current jth neuron. V_{th} is the threshold for the neuron to fire a signal. $S_i(t)$ and $S_j(t)$ are input and the resulting output spike trains of current neuron, respectively. The firing signals are generated as follow:

$$S_j(t) = \begin{cases} 1, & \text{if } V_j'(t) \geq V_{th} \\ 0, & \text{otherwise.} \end{cases} \tag{2}$$

where $V_j'(t) = V_j(t-1) + V_{th} \sum^{\mathcal{N}_j} w_{ij}^s S_i(t)$ denotes the membrane potential before signal firing and potential reset operation.

Considering ANN-SNN conversion and rate-based coding, we can compute spike rate as $r = \sum_{t=1}^{T} S(t)/T$ for a total timestep T. The goal of a conversion process is to derive a function transfers the parameters of an ANN to the SNN as $w^s = f(w^a)$ so that each neuron in the SNN produces a spike rate $r \propto a$ after T timesteps, where a is the corresponding activation value of original networks.

To this end, we can derive the spike count of the output spike train by summing Eqn. 1 over total timesteps T:

$$\sum_{t=1}^{T} S_j(t) = \sum_{i \in \mathcal{N}_j} w_{ij}^s \sum_{t=1}^{T} S_i(t) - \frac{V_j(T) - V_j(1)}{V_{th}}, \tag{3}$$

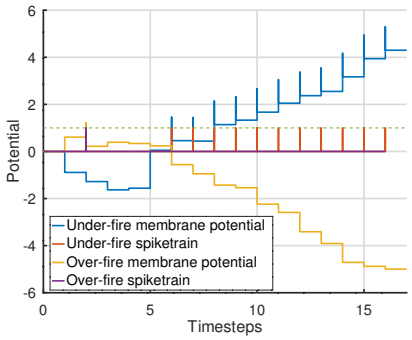

(a) Over-fire and under-fire phenomenons

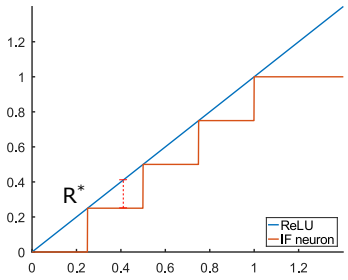

(b) ReLU and IF neuron.

Figure 1: For each step of the membrane potential line in the figure, the left horizontal line indicates $V(t-1)$. The peak point indicates $V'(t)$, and the right horizontal line indicates $V(t)$ which is transferred to the next step. For over-fire spike train(purple), $\sum_{t=1}^{T} S_j(t) = 1$ while $\sum_{t=1}^{T} S_j^*(t) = 0$. For under-fire spike train(orange), $\sum_{t=1}^{T} S_j(t) = 11$ while $\sum_{t=1}^{T} S_j^*(t) = 15$.

where $V_j(1)$ is the initial membrane potential. For convenience, we set $V_j(1) = 0$ in this work without loss of generality. Eqn. 3 gives the relation between the total spike count of current neuron and its input neurons' spike count besides the internal membrane potential.

For an ideal conversion, the spiking neuron intergrates membrane potential uniformly accross time and introduces no error during inference. Under this ideal condition, the output spike count should fullfill the following equation,

$$\sum_{t=1}^{T} S_j^*(t) = \left\lfloor \max\left(\frac{V_a}{V_{th}}, 0\right) \right\rfloor, \tag{4}$$

where $V_a = V_{th} \sum_{i \in \mathcal{N}_j} w_{ij}^s \sum_{t=1}^{T} S_i(t)$ denotes the accumulated membrane potential. Please refer to the appedix for detail proof. Assuming Eqn. 4 hold, we can derive the ideal output spike rate by averaging Eqn. 4 over timesteps T:

$$r_j^* = \max\left(\sum_{i \in \mathcal{N}_j} w_{ij}^s r_i, 0\right) - R^*. \tag{5}$$

where R^* is defined as follow.

$$R^* = \begin{cases} \frac{\frac{V_a}{V_{th}} - \lfloor \frac{V_a}{V_{th}} \rfloor}{T}, & \text{if } V_a > 0 \\ 0, & \text{otherwise.} \end{cases} \tag{6}$$

For the ideal ANN-SNN conversion situation, when R^* is approaching zero, the formal expression of a simple IF neuron becomes similar to the ReLU function in processing information. Thus, the weight of a SNN can be transformed from its counterpart ANN directly. Since spike rate r^* is bounded, a linear mapping function is utilized to convert ANN weights $W^s = f(W^a) = \frac{\lambda_i}{\lambda_j} W^a$, in which λ_i is the scale factor for layer i.

3.1.1 Coding Error

As shown in Eqn. 5, R^* can be viewed as a *coding error* term for the ideal conversion process during the ANN-SNN weight mapping. As $\frac{V_a}{V_{th}} - \left\lfloor \frac{V_a}{V_{th}} \right\rfloor < 1$ for $V_a > 0$, the upper bound of the conversion error $R^* < 1/T$ continuously decreases when the timesteps is set increasingly. Due to errors accumulated between layers, the converted SNNs with deep layers require large timesteps T to maintain high fidelity and performance [39, 23]. On the other hand, the large timesteps impair the efficiency of the SNN. This phenomenon is also known as accuracy-latency trade-off [9, 31].

3.1.2 Inference Error

Besides the conversion error, the assumption in Eqn. 4 can be contravened easily due to essential nature of SNN neurons during the inference. Intuitively, the inference process of SNN is quite dynamic and spiking neurons are unable to accumulate membraine potential uniformly accross timesteps as Eqn. 4, which leads to the divergence of overall output spike counts. We refer to this type of error as *inference error*.

We conclude two situations where the Eqn. 4 is violated during inference: over-fire and under-fire phenomenons. Over-fire indicates the situation where number of total generated spikes is greater than number of expected spikes $\sum_{t=1}^{T} S_j(t) > \sum_{t=1}^{T} S_j^*(t)$. Volatile membrane potential may cross the threshold $V_j'(t) \geq V_{th}$ and cause spike $S_j(t) = 1$ that makes the number of generating spikes exceeding the number of expected spikes. Conversely, under-fire refers to the situation where insufficient spikes have been generated $\sum_{t=1}^{T} S_j(t) < \sum_{t=1}^{T} S_j^*(t)$. With inadequate spikes, under-fire neurons will have membrane potential large than V_{th} at the end of inference. Fig. 1a shows an example of these two situations.

3.2 Quantized ReLU Activation

To deal with the coding error, we propose a Quantized ReLU activation function in ANN training stage to accurately transform the weights to SNN with limited timesteps. According to Eqn.4, we can reformulate Eqn. 5 in a different way :

$$r_j^* = \frac{\left\lfloor T \max(\sum^{\mathcal{N}_j} w_{ij}^s r_i, 0) \right\rfloor}{T}. \tag{7}$$

Let $x_s = \sum^{\mathcal{N}_j} w^s r_i$ be the weighted sum of input spike rates in SNNs. Taking maximal spike rate into consideration, IF neuron(Fig. 1b) can be described with step function as follow,

$$IF(x_s) = \begin{cases} 0, & \text{if } x_s \leq 0 \\ r^{max}, & \text{if } x_s \geq r^{max} \\ \frac{\lfloor T x_s \rfloor}{T} & \text{otherwise.} \end{cases} \tag{8}$$

The r^{max} is the maximum spike rate of a spike train, which is 1 for conventional spike trains. The proposed function is strictly equivalent to the IF neuron instead of increasing total timesteps T to approximate the ReLU function with a fine-grain step function. By mapping spike rate and activation value $a = \lambda r$, the proposed activation function is derived through Eqn. 8 :

$$QReLU(x_a, \lambda) = \lambda IF(\frac{x_a}{\lambda}) = \begin{cases} 0, & \text{if } x_a \leq 0 \\ \lambda, & \text{if } x_a \geq \lambda \\ \frac{\lfloor \frac{T}{\lambda} x_a \rfloor}{\frac{T}{\lambda}}, & \text{otherwise.} \end{cases} \tag{9}$$

We name the proposed activation function as QReLU, since it can be seen as a quantized version of the ReLU function. The approximate gradients are given by the PACT algorithm [6] originated from STE [1]:

$$\frac{\partial QReLU(x_a, \lambda)}{\partial \lambda} = \begin{cases} 0, & \text{if } x_a < \lambda \\ 1, & \text{otherwise.} \end{cases} \tag{10}$$

$$\frac{\partial QReLU(x_a, \lambda)}{\partial x_a} = \begin{cases} 1, & \text{if } 0 < x_a < \lambda \\ 0, & \text{otherwise.} \end{cases} \tag{11}$$

The scale factor λ here is also referred to as quantization boundary and is learned during the ANN training process. Guaranteed by the success of quantization techniques [1, 6], a neural network consisting of QReLU is capable of achieving similar performance compared to the original ANN. By

mapping weights from an ANN equiped with QReLU activation, the coding error R^* is eliminated in theory.

3.3 Buffered Non-leaky IF Neuron

For the inference error, we observe that reduing over-fire problem alone can boost performance siginificantly based on our experiments. To further improve our conversion framework, we propose a novel buffered non-leaky IF neuron to relieve the over-fire situation to compensate for the inference errors.

The proposed buffered neuron utilizes a recurrent mechanism to regulate the spikes. In the proposed neuron, an additional buffered potential V^b is introduced as follows:

$$V_j^b(t) = V_j^b(t-1) + V_{th} S_j(t). \tag{12}$$

Similar to the membrane potential, the initial buffer potential $V_j^b(1)$ is set to zero for convenience. The spike generating process is described as

$$S_j(t) = \begin{cases} 1, & \text{if } V_j'(t) > V_{th} \\ -1, & \text{if } V_j'(t) < 0 \text{ and } V_j^b(t-1) \geq V_{th} \\ 0, & \text{otherwise.} \end{cases} \tag{13}$$

Intuitively, the proposed Buffered Non-leaky IF Neuron generates negative spikes to regulate the total spikes count for the inference errors. Thus, the over-fire problem can be alleviated. Please refer to appendix for detail proof. As same as ordinary IF neurons, only addition operation and threshold functions are involved in the proposed neuron. The inference efficiency is preserved since the extra power required by transmitting sign bit between neurons is negligible [45].

3.4 Integration with Multiple Bits Spike Train

To further improve the performance of the proposed conversion framework, we integrate shift-based multi-bits spike train into the proposed framework. Unlike the previous work [45] which compressed an existing SNN to speed up the inference, we extend the definition of the spike as $S(t) \in \{2^n | n \in \mathbb{N}, 2^n \leq S^{max}\}$ to facilitate the shift operation directly during the conversion. The multi-bits spike train version of Eqn.13 is as follow:

$$S_j(t) = \begin{cases} A(\left\lfloor \frac{V_j'(t)}{V_{th}} \right\rfloor), & \text{if } V_j'(t) > V_{th} \\ A(\min\left(\left\lfloor \frac{V_j'(t)}{-V_{th}} \right\rfloor, \left\lfloor \frac{V_j^b(t-1)}{V_{th}} \right\rfloor \right)), & \text{if } V_j'(t) < 0 \text{ and } V_j^b(t) \geq V_{th} \\ 0, & \text{otherwise,} \end{cases} \tag{14}$$

where the adjust function $A(\cdot)$ is defined as

$$A(x) = 2^{\lfloor \log_2(\min(x, S^{max})) \rfloor}. \tag{15}$$

Multiple bits spike train carries more information than ubiquitous on-off spikes [5, 22, 33, 47]. However, expensive multiplications are required during the integration with non-uniform spikes. To avoid multiplication, we employ the log_2 adjust function and shift operation [45] as an alternative and achieve high energy efficiency. The adjust function can be implemented with a conditional function.

For QReLU, as the maximal ratio coding is equal to maximal spike counts, $r^{max} = \sum_{t=1}^{T} S^{max}/T = S^{max}$, the multi-bits version of Eqn. 9 can be described as follow:

Table 1: Classification performance compared to other methods in CIFAR10 and ImageNet-1k

Model	Arch	SNN Top-1	Δ	T
CIFAR10				
Rueckauer et al. [39]	4 Conv, 2 Linear	90.85%	-1.06%	400
Sengupta et al. [40]	ResNet20	87.46%	-1.64%	2500
Lee et al. [26]	VGG9	90.45%	-	100
Kim and Panda [24]	VGG9	90.50%	-	25
Wu et al. [43]	5 Conv, 2 Linear	90.53%	-	12
Han et al. [16]	ResNet20	91.36%	-0.11%	2048
Rathi et al. [37]	ResNet20	92.22%	-0.93%	250
Rathi and Roy [36]	ResNet20	92.14%	-0.65%	25
Zheng et al. [48]	ResNet19	93.16%	-	6
Yu et al. [47]	6 Conv, 2 Linear	93.90%	-0.23%	300
Yan et al. [46]	VGG19	92.48%	-0.08%	600
Deng and Gu [8]	ResNet20	92.41%	0.09%	16
Ding et al. [10]	PreActResNet18	91.96%	-1.10%	64
Bu et al. [3]	ResNet18	94.82%	-1.22%	8
Bu et al. [3]	ResNet18	95.92%	-0.12%	16
Ours	**ResNet18**	**95.13%**	**-0.17%**	**8**
Ours	**ResNet18**	**95.14%**	**-0.04%**	**16**

Model	Arch	SNN Top-1	Δ	T
ImageNet				
Rueckauer et al. [39]	VGG16	49.61%	-14.28%	400
Sengupta et al. [40]	VGG16	69.96%	-0.56%	2500
Han et al. [16]	VGG16	73.09%	-0.40%	4096
Rathi et al. [37]	VGG16	65.19%	-4.16%	250
Rathi and Roy [36]	VGG16	66.52%	-3.56%	25
Deng and Gu [8]	VGG16	55.80%	-16.6%	16
Bu et al. [3]	VGG16	50.97%	-23.32%	16
Bu et al. [3]	VGG16	68.47%	-5.82%	32
Ours	**VGG16**	**73.65%**	**-1.69%**	**8**
Ours	**VGG16**	**75.96%**	**-0.07%**	**16**
Sengupta et al. [40]	ResNet34	65.47%	-5.22%	2000
Han et al. [16]	ResNet34	65.47%	%	4096
Fang et al. [14]	ResNet34	67.04%	-	4
Zheng et al. [48]	ResNet34	63.72%	-	6
Li et al. [27]	ResNet34	64.51%	-11.12%	32
Li et al. [27]	ResNet34	74.61%	-1.05%	256
Bu et al. [3]	ResNet34	59.35%	-14.97%	16
Bu et al. [3]	ResNet34	69.37%	-4.95%	32
Ours	**ResNet34**	**73.20%**	**-0.52%**	**8**
Ours	**ResNet34**	**74.46%**	**0.08%**	**16**

Table 2: Detection performance

Model	Arch	SNN AP50	Δ	T
PASCAL VOC				
Kim et al. [23]	tiny-yolo	51.83%	-1.18%	5000
Ours	**tiny-yolo**	**65.20%**	**-0.13%**	**16**
Ours	**tiny-yolo**	**65.73%**	**-0.06%**	**32**
MS COCO				
Kim et al. [23]	tiny-yolo	25.66%	-0.58%	5000
Ours	**tiny-yolo**	**38.6%**	**-1.1%**	**16**
Ours	**tiny-yolo**	**39.2%**	**-0.6%**	**32**

Table 3: SNN computation efficiency.

Methods	Architecture (timesteps)	Operation ratio	SNN/ANN energy ratio
CIFAR10			
Rathi and Roy [36]	ResNet20(25)	2.55	0.51
Ours	ResNet18(8)	0.92	0.19
Ours	ResNet18(16)	1.69	0.34
ImageNet			
Rathi and Roy [36]	VGG16(25)	1.62	0.32
Ours	VGG16(8)	1.92	0.39
Ours	VGG16(16)	3.03	0.62

$$QReLU(x_a, \lambda^b) = \begin{cases} 0, & \text{if } x_a \leq 0 \\ \lambda^b, & \text{if } x_a \geq \lambda^b \\ \frac{\lfloor \frac{P}{\lambda^b} x_a \rfloor}{\frac{P}{\lambda^b}}, & \text{otherwise.} \end{cases} \tag{16}$$

Here the $\lambda^b = \lambda S^{max}$ is the quantization boundary and $P = TS^{max}$ is the *representation power*. As implied by the definition of the representation power, even the minimal shift extension with $S^{max} = 2$ can maintain the same representation power with half timesteps. This phenomenon is named *strength-latency trade-off*.

4 Experiments

In this section, we conduct experiments on both classification and detection tasks to demonstrate the efficiency and effectiveness of the proposed method. Since the equivalency of features and spike rates are universal throughout the entire network, real-valued input is directly utilized in the converted SNN. We select a unity threshold $V_{th} = 1$ for all our experiments. Max spike value $S^{max} = 2$ is used for all experiments if not stated otherwise. Other implementation details can be found in the appendix.

4.1 Visual Object Recognition and Detection Performance

We test our proposed High Performance Conversion framework (HPC) on visual object recognition and detection tasks. A ResNet18 [17] like architecture is utilized as backbone networks to conduct experiments on the CIFAR10 [25] dataset and a VGG16 [41] like network is trained on the ImageNet [7] dataset. Table 1 reports the classification accuracy of the proposed HPC compared

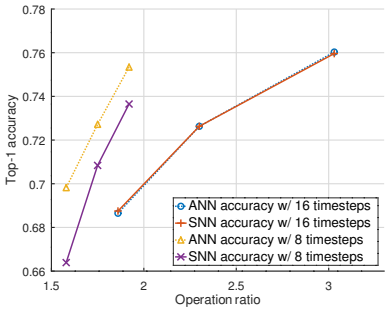

Operation ratio

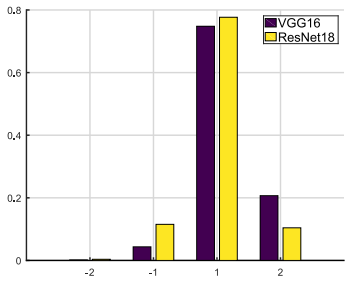

Distribution of spike values.

Figure 2: Left: Operation ratio and performance with ImageNet dataset under 16 timesteps. Data points with same operation ratio are converted SNN and its corresbonding ANN. Right: Distribution of spike values.

with other methods. Top-1 accuracy is used to evaluate the performance. Since the performance of converted SNN is closely related to the ANN baseline, a performance drop Δ is also reported. As illustrated in Table 1, the proposed HPC can perform nearly lossless conversion while maintaining low inference latency.

As a general method, we also test our HPC with tiny-yolo [38] structure on both PASCAL VOC [13] and MS COCO [28] datasets. Table 2 summarizes the AP50 performance of the proposed method. We can see that our proposed HPC can achieve state-of-the-art conversion performance within 32 timesteps, which is over 100 times faster than the previous SNN detection work [23].

4.2 Energy Efficiency

To evaluate the energy efficiency of the proposed method, *operation ratio* is adopted to measure the overall efficiency as described in Eqn. 17. In contrast to actual energy consumption which may vary between hardware devices [32], counting-based metric [36] is straightforward and representative for different methods. For a fair comparison, integration operations triggered by spikes for both membrane potential and buffer potential are counted in our experiments.

$$\textit{operation ratio} = \frac{\#(\text{addition ops in SNN})}{\#(\text{flops in ANN})}. \tag{17}$$

Operation ratios, as well as estimated energy consumption ratio, are summarized in Table 3. Here we roughly estimate that multiplication consumes 4 times more energy than addition according to Horowitz [18]. The results on the CIFAR10 dataset show a strong correlation between timesteps and energy efficiency. To further study energy efficiency, we test the relationship between operation ratio and networks performance. As depicted in Fig. 2a, under the same timesteps setting, the spike ratio continuously decreases with the overall performance. Our experiments confirm a general relationship between inference energy and performance, which holds even under constant latency.

Fig. 2b depicts the distributions of spike values in classification experiments. Without loss of generality, we conclude that only 20% of the spikes require shift operation. As measured by Gudovskiy and Rigazio [15], the shift operation only cost 10% of energy consumed by addition operation. Thus, multi-bits spike only use 2% extra energy, which is negligible.

4.3 Ablation Study

To reveal the effectiveness of the proposed framework, we conduct ablation studies on both classification and detection tasks. Specifically, we remove the quantized training technique and the buffered IF neuron sequentially and compare the results. The baseline ANN is trained and fixed for experiments without QReLU component, meanwhile quantized ANN networks are trained separately for different timestep configurations. Without the QReLU, the scale factor is calculated using the percentile function with the parameter empirically set to 99.0. Channel-wise normalization is utilized to ensure competitive performances. Since conventional converted SNN requires large timesteps to

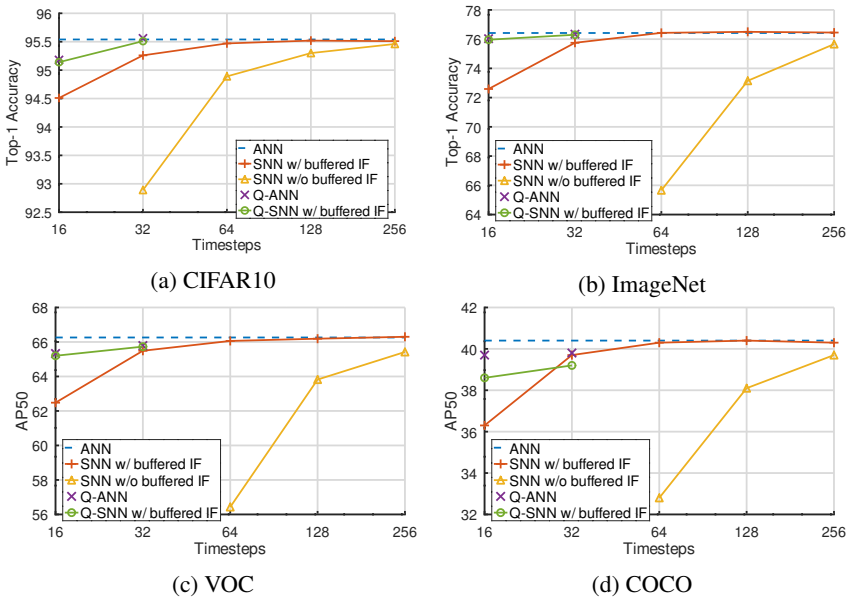

(a) CIFAR10 (b) ImageNet

(c) VOC (d) COCO

Figure 3: Ablation study of proposed techniques. Q-ANN denotes ANNs trained with QReLU, Q-SNN denotes SNNs converted from ANN trained with QReLU. SNN w/ buffered IF means that buffered non-leaky integrated and fire neuron are used. SNN w/o buffered IF are conventional SNNs with out the proposed neuron.

achieve plausible performance, we only report those performances with 32 or more timesteps for the CIFAR10 dataset and 64 for others.

Fig. 3 validates the effectiveness of the proposed techniques. Compared to conventional SNNs, the SNN integrates with buffered neurons only requires a quarter of timesteps to reach the same performance. As the buffered neuron mitigates only the over-fire problem, we conclude that the over-fire situation is the primary cause of performance degradation during inference. The introduction of quantized training further enhances the performance of converted SNN under limited timesteps. Similar trends can be observed across experiments.

5 Conclusion and Limitation

In this paper, we proposed a novel High Performance Conversion (HPC) method to simultaneously achieve high-performance SNN inference with low latency. Efforts had been made to reduce both coding errors and often overlooked inference errors. A novel QReLU activation was proposed to eliminates the conversion error. Meanwhile, a buffered non-leaky IF neuron was designed to mitigate the over-fire problem and boost the inference performance while maintaining its simplicity and efficiency. For the first time, efficient SNN converted without extra fine-tuning revealed its capability to achieve state-of-the-art performances in nontrivial vision tasks.

However, there are limitations. Since no actual hardware is involved, the efficiency is estimated using energy consumed by simple operations. As computing platform evolves rapidly, it is beyond our reach to accomplish real neuromorphic hardware which can be researched in further work.

For furture work, we believe further study on novel structures such as attention mechanisms SE [19] and transformer [12] can extend the current framework and may lead to better understanding of the underlying perception mechanism. Moreover, applications of SNN on video-like input that achieves ANN level performance with great efficiency are another promising direction.

References

[1] Y. Bengio, N. Léonard, and A. Courville. Estimating or propagating gradients through stochastic neurons for conditional computation. *CoRR*, 2013.

[2] S. M. Bohte, J. N. Kok, and H. La Poutré. Error-backpropagation in temporally encoded networks of spiking neurons. *Neurocomputing*, 48(1):17 – 37, 2002. ISSN 0925-2312. doi: 10.1016/S0925-2312(01)00658-0.

[3] T. Bu, W. Fang, J. Ding, P. DAI, Z. Yu, and T. Huang. Optimal ANN-SNN conversion for high-accuracy and ultra-low-latency spiking neural networks. In *International Conference on Learning Representations*, 2022.

[4] Y. Cao, Y. Chen, and D. Khosla. Spiking deep convolutional neural networks for energy-efficient object recognition. *International Journal of Computer Vision*, 113(1):54–66, May 2015. ISSN 1573-1405. doi: 10.1007/s11263-014-0788-3.

[5] R. Chen, H. Ma, S. Xie, P. Guo, P. Li, and D. Wang. Fast and efficient deep sparse multi-strength spiking neural networks with dynamic pruning. In *2018 International Joint Conference on Neural Networks (IJCNN)*, pages 1–8, 2018. doi: 10.1109/IJCNN.2018.8489339.

[6] J. Choi, Z. Wang, S. Venkataramani, P. I.-J. Chuang, V. Srinivasan, and K. Gopalakrishnan. Pact: Parameterized clipping activation for quantized neural networks. *CoRR*, 2018.

[7] J. Deng, W. Dong, R. Socher, L. Li, Kai Li, and Li Fei-Fei. Imagenet: A large-scale hierarchical image database. In *2009 IEEE Conference on Computer Vision and Pattern Recognition*, pages 248–255, 2009. doi: 10.1109/CVPR.2009.5206848.

[8] S. Deng and S. Gu. Optimal conversion of conventional artificial neural networks to spiking neural networks. In *International Conference on Learning Representations*, 2021.

[9] P. U. Diehl, D. Neil, J. Binas, M. Cook, S. Liu, and M. Pfeiffer. Fast-classifying, high-accuracy spiking deep networks through weight and threshold balancing. In *2015 International Joint Conference on Neural Networks (IJCNN)*, pages 1–8, 2015. doi: 10.1109/IJCNN.2015.7280696.

[10] J. Ding, Z. Yu, Y. Tian, and T. Huang. Optimal ann-snn conversion for fast and accurate inference in deep spiking neural networks. In *IJCAI*, 2021. doi: 10.24963/ijcai.2021/321.

[11] S. Dong, T. Huang, and Y. Tian. Spike camera and its coding methods. In *Data Compression Conference (DCC)*, 2017.

[12] A. Dosovitskiy and et al. An image is worth 16x16 words: Transformers for image recognition at scale. In *ICLR*, 2021.

[13] M. Everingham, L. Van Gool, C. K. I. Williams, J. Winn, and A. Zisserman. The pascal visual object classes (voc) challenge. *International Journal of Computer Vision*, 2010. doi: 10.1007/s11263-009-0275-4.

[14] W. Fang, Z. Yu, Y. Chen, T. Huang, T. Masquelier, and Y. Tian. Deep residual learning in spiking neural networks. In A. Beygelzimer, Y. Dauphin, P. Liang, and J. W. Vaughan, editors, *Advances in Neural Information Processing Systems*, 2021.

[15] D. Gudovskiy and L. Rigazio. Shiftcnn: Generalized low-precision architecture for inference of convolutional neural networks. *CoRR*, 2017.

[16] B. Han, G. Srinivasan, and K. Roy. Rmp-snn: Residual membrane potential neuron for enabling deeper high-accuracy and low-latency spiking neural network. In *CVPR*, 2020.

[17] K. He, X. Zhang, S. Ren, and J. Sun. Deep residual learning for image recognition. In *Proceedings of the IEEE Conference on Computer Vision and Pattern Recognition (CVPR)*, June 2016.

[18] M. Horowitz. 1.1 computing's energy problem (and what we can do about it). In *2014 IEEE International Solid-State Circuits Conference Digest of Technical Papers (ISSCC)*, pages 10–14, 2014. doi: 10.1109/ISSCC.2014.6757323.

[19] J. Hu, L. Shen, and G. Sun. Squeeze-and-excitation networks. In *CVPR*, pages 7132–7141, 2018. doi: 10.1109/CVPR.2018.00745.

[20] D. Huh and T. J. Sejnowski. Gradient descent for spiking neural networks. In S. Bengio, H. Wallach, H. Larochelle, K. Grauman, N. Cesa-Bianchi, and R. Garnett, editors, *Advances in Neural Information Processing Systems*, volume 31, pages 1433–1443. Curran Associates, Inc., 2018.

[21] Y. Jin, W. Zhang, and P. Li. Hybrid macro/micro level backpropagation for training deep spiking neural networks. In S. Bengio, H. Wallach, H. Larochelle, K. Grauman, N. Cesa-Bianchi, and

R. Garnett, editors, *Advances in Neural Information Processing Systems*, volume 31, pages 7005–7015. Curran Associates, Inc., 2018.

[22] J. Kim, H. Kim, S. Huh, J. Lee, and K. Choi. Deep neural networks with weighted spikes. *Review of Economic Dynamics*, 311:373–386, Oct. 2018. ISSN 1094-2025. doi: 10.1016/j.neucom.2018.05.087. Funding Information: This work was supported by the KIST Institutional Program (Project No. 2E27330-17-P026).

[23] S. Kim, S. Park, B. Na, and S. Yoon. Spiking-yolo: Spiking neural network for energy-efficient object detection. *AAAI*, 2020.

[24] Y. Kim and P. Panda. Revisiting batch normalization for training low-latency deep spiking neural networks from scratch, 2020.

[25] A. Krizhevsky, G. Hinton, et al. Learning multiple layers of features from tiny images. *Tech Report*, 2009.

[26] C. Lee, S. S. Sarwar, P. Panda, G. Srinivasan, and K. Roy. Enabling spike-based backpropagation for training deep neural network architectures. *Frontiers in Neuroscience*, 14, Feb 2020. ISSN 1662-453X. doi: 10.3389/fnins.2020.00119.

[27] Y. Li, S. Deng, X. Dong, R. Gong, and S. Gu. A free lunch from ann: Towards efficient, accurate spiking neural networks calibration. In *ICML*, pages 6316–6325, 2021.

[28] T.-Y. Lin, M. Maire, S. Belongie, J. Hays, P. Perona, D. Ramanan, P. Dollár, and C. L. Zitnick. Microsoft coco: Common objects in context. In *ECCV*, 2014. ISBN 978-3-319-10602-1.

[29] H. Mostafa. Supervised learning based on temporal coding in spiking neural networks. *IEEE Transactions on Neural Networks and Learning Systems*, 29(7):3227–3235, 2018. doi: 10.1109/TNNLS.2017.2726060.

[30] E. O. Neftci, H. Mostafa, and F. Zenke. Surrogate gradient learning in spiking neural networks: Bringing the power of gradient-based optimization to spiking neural networks. *IEEE Signal Processing Magazine*, 36(6):51–63, 2019. doi: 10.1109/MSP.2019.2931595.

[31] D. Neil, M. Pfeiffer, and S.-C. Liu. Learning to be efficient: Algorithms for training low-latency, low-compute deep spiking neural networks. In *Proceedings of ACM Symposium on Applied Computing*, 2016.

[32] D. E. Nikonov and I. A. Young. Benchmarking physical performance of neural inference circuits. *CoRR*, 2019.

[33] S. Park, S. Kim, H. Choe, and S. Yoon. Fast and efficient information transmission with burst spikes in deep spiking neural networks. In *2019 56th ACM/IEEE Design Automation Conference (DAC)*, pages 1–6, 2019.

[34] N. Perez-Nieves and D. Goodman. Sparse spiking gradient descent. In M. Ranzato, A. Beygelzimer, Y. Dauphin, P. Liang, and J. W. Vaughan, editors, *Advances in Neural Information Processing Systems*, volume 34, pages 11795–11808. Curran Associates, Inc., 2021.

[35] J. A. Pérez-Carrasco, B. Zhao, C. Serrano, B. Acha, T. Serrano-Gotarredona, S. Chen, and B. Linares-Barranco. Mapping from frame-driven to frame-free event-driven vision systems by low-rate rate coding and coincidence processing–application to feedforward convnets. *IEEE Transactions on Pattern Analysis and Machine Intelligence*, 35(11):2706–2719, 2013. doi: 10.1109/TPAMI.2013.71.

[36] N. Rathi and K. Roy. Diet-snn: Direct input encoding with leakage and threshold optimization in deep spiking neural networks. *CoRR*, 2020.

[37] N. Rathi, G. Srinivasan, P. Panda, and K. Roy. Enabling deep spiking neural networks with hybrid conversion and spike timing dependent backpropagation. In *International Conference on Learning Representations*, 2020.

[38] J. Redmon, S. Divvala, R. Girshick, and A. Farhadi. You only look once: Unified, real-time object detection. In *CVPR*, June 2016.

[39] B. Rueckauer, I. Lungu, Y. Hu, M. Pfeiffer, and S. Liu. Conversion of continuous-valued deep networks to efficient event-driven networks for image classification. *Frontiers in Neuroscience*, 2017. ISSN 1662-453X. doi: 10.3389/fnins.2017.00682.

[40] A. Sengupta, Y. Ye, R. Wang, C. Liu, and K. Roy. Going deeper in spiking neural networks: Vgg and residual architectures. *Frontiers in Neuroscience*, 13:95, 2019. ISSN 1662-453X. doi: 10.3389/fnins.2019.00095.

[41] K. Simonyan and A. Zisserman. Very deep convolutional networks for large-scale image recognition. In Y. Bengio and Y. LeCun, editors, *3rd International Conference on Learning Representations*, 2015.

[42] J. C. Thiele, O. Bichler, and A. Dupret. Spikegrad: An ann-equivalent computation model for implementing backpropagation with spikes. In *International Conference on Learning Representations*, 2020.

[43] Y. Wu, L. Deng, G. Li, J. Zhu, Y. Xie, and L. Shi. Direct training for spiking neural networks: Faster, larger, better. *Proceedings of the AAAI Conference on Artificial Intelligence*, 33(01): 1311–1318, Jul. 2019. doi: 10.1609/aaai.v33i01.33011311.

[44] F. Xing, Y. Yuan, H. Huo, and T. Fang. Homeostasis-based cnn-to-snn conversion of inception and residual architectures. In T. Gedeon, K. W. Wong, and M. Lee, editors, *Neural Information Processing*, pages 173–184, Cham, 2019. Springer International Publishing. ISBN 978-3-030-36718-3.

[45] C. Xu, W. Zhang, Y. Liu, and P. Li. Boosting throughput and efficiency of hardware spiking neural accelerators using time compression supporting multiple spike codes. *Frontiers in Neuroscience*, 14:104, 2020. ISSN 1662-453X. doi: 10.3389/fnins.2020.00104.

[46] Z. Yan, J. Zhou, and W.-F. Wong. Near lossless transfer learning for spiking neural networks. *Proceedings of the AAAI Conference on Artificial Intelligence*, 35(12):10577–10584, May 2021.

[47] Q. Yu, C. Ma, S. Song, G. Zhang, J. Dang, and K. C. Tan. Constructing accurate and efficient deep spiking neural networks with double-threshold and augmented schemes, 2020.

[48] H. Zheng, Y. Wu, L. Deng, Y. Hu, and G. Li. Going deeper with directly-trained larger spiking neural networks. *Proceedings of the AAAI Conference on Artificial Intelligence*, 35(12): 11062–11070, May 2021.

Checklist

The checklist follows the references. Please read the checklist guidelines carefully for information on how to answer these questions. For each question, change the default **[TODO]** to [Yes] , [No] , or [N/A] . You are strongly encouraged to include a **justification to your answer**, either by referencing the appropriate section of your paper or providing a brief inline description. For example:

- Did you include the license to the code and datasets? [Yes] See Section **??**.
- Did you include the license to the code and datasets? [No] The code and the data are proprietary.
- Did you include the license to the code and datasets? [N/A]

Please do not modify the questions and only use the provided macros for your answers. Note that the Checklist section does not count towards the page limit. In your paper, please delete this instructions block and only keep the Checklist section heading above along with the questions/answers below.

1. For all authors...
   (a) Do the main claims made in the abstract and introduction accurately reflect the paper's contributions and scope? [Yes]
   (b) Did you describe the limitations of your work? [Yes]
   (c) Did you discuss any potential negative societal impacts of your work? [No]
   (d) Have you read the ethics review guidelines and ensured that your paper conforms to them? [Yes]
2. If you are including theoretical results...
   (a) Did you state the full set of assumptions of all theoretical results? [Yes]
   (b) Did you include complete proofs of all theoretical results? [Yes]

3. If you ran experiments...
   (a) Did you include the code, data, and instructions needed to reproduce the main experimental results (either in the supplemental material or as a URL)? [No] Source code will be released later.
   (b) Did you specify all the training details (e.g., data splits, hyperparameters, how they were chosen)? [Yes] Training details can be found in the appendix.
   (c) Did you report error bars (e.g., with respect to the random seed after running experiments multiple times)? [Yes] Performance stability is reported in the appendix.
   (d) Did you include the total amount of compute and the type of resources used (e.g., type of GPUs, internal cluster, or cloud provider)? [Yes] Training details can be found in the appendix.
4. If you are using existing assets (e.g., code, data, models) or curating/releasing new assets...
   (a) If your work uses existing assets, did you cite the creators? [Yes]
   (b) Did you mention the license of the assets? [No] Popular datasets are used.
   (c) Did you include any new assets either in the supplemental material or as a URL? [No]
   (d) Did you discuss whether and how consent was obtained from people whose data you're using/curating? [N/A]
   (e) Did you discuss whether the data you are using/curating contains personally identifiable information or offensive content? [N/A]
5. If you used crowdsourcing or conducted research with human subjects...
   (a) Did you include the full text of instructions given to participants and screenshots, if applicable? [N/A]
   (b) Did you describe any potential participant risks, with links to Institutional Review Board (IRB) approvals, if applicable? [N/A]
   (c) Did you include the estimated hourly wage paid to participants and the total amount spent on participant compensation? [N/A]